

# Complex Shift Dynamics of Some Elementary Cellular Automaton Rules

**Junbiao Guan**

*School of Science, Hangzhou Dianzi University  
Hangzhou, Zhejiang 310018, P.R. China  
junbiaoguan@gmail.com*

**Kaihua Wang**

*School of Mathematics and Statistics  
Hainan Normal University  
Haikou, Hainan 571158, P.R. China*

---

This paper presents a discussion of complex shift dynamics of some elementary cellular automaton rules (rules 30, 41, and 110). Equations that show some degree of self-similarity are obtained. It is demonstrated that rules 30, 41, and 110 exhibit Bernoulli shifts and are topologically mixing on one of their own closed invariant subsystems. Furthermore, many complex Bernoulli shifts are explored for finite symbolic sequences with periodic boundary conditions.

---

## 1. Introduction

It is natural to study a dynamical system either directly or via other equivalent systems that are better understood. Another good way to study a dynamical system is through its subsystems, which may also to some extent help to understand its dynamical properties. Symbolic representations are methods for studying dynamical systems through shifts and subshifts [1, 2]. It is well known that shifts and subshifts defined on a space of abstract symbols are special discrete dynamical systems called *symbolic* dynamical systems. Symbolic dynamics, as a powerful tool for studying more general discrete dynamical systems, often contain invariant subsets on which the dynamics are similar or even equivalent to a shift or subshift.

Cellular automata are spatially and temporally discrete dynamical systems characterized by local interactions [3, 4]. Such systems can be better investigated if each rule is assigned to an interval map [5–8]. The construction of the interval map associated to a cellular automaton rule depends on the choice of an underlying subshift of finite type, say, a cellular automaton rule, that accounts for the configurational space, and depends on the choice of the interval map implementing the subshift of finite type. If we choose subshifts of finite type that are

invariant for cellular automata, we obtain some simple interval maps that can be presented in a closed form.

Motivated by the cited works, the aim of this paper is to explore complex shift dynamics of some special elementary cellular automaton rules, in particular rules 30, 41, and 110, from the viewpoint of symbolic dynamics. The structure of the remainder of the paper is as follows: Section 2 provides some notations and definitions. Section 3 focuses on the discussion of complex shift dynamical properties of rules 30, 41, and 110. By associating these rules with the interval maps defined in  $[0, 1]$ , it is shown that the interval maps exhibit some degree of self-similarity. Based on directed graph theory, it is demonstrated that rules 30, 41, and 110 exhibit Bernoulli shifts and are topologically mixing on one of their own closed invariant subsystems. Moreover, many complex Bernoulli shifts are explored for the finite symbolic sequences with periodic boundary conditions. Finally, Section 4 concludes the text of this paper.

## 2. Preliminaries

Before turning to Section 3 to investigate the complex shift dynamics of hyper Bernoulli-shift rules 30, 41, and 110, we shall introduce some notations and recall some definitions.

Let  $\mathcal{A}$  be a finite set. For a finite alphabet  $\mathcal{A} = \{0, 1, \dots, r\}$ , denote by  $\mathcal{A}^* := \bigcup_{n \geq 0} \mathcal{A}^n$  the set of words over  $\mathcal{A}$ . The length of a word  $\xi \in \mathcal{A}^n$  is denoted by  $|\xi| := n$ . We say that  $\xi \in \mathcal{A}^*$  appears in  $x \in \mathcal{A}^*$  if there exists  $k$  such that  $x_{k+i} = \xi_i$  for all  $i < |\xi|$ . We denote by  $\xi_{[i,j]} = \xi_i \dots \xi_j$  subwords of  $\xi$  associated with intervals. Let  $\mathcal{A}^{\mathbb{Z}} = \{\xi = (\xi_i)_{i \in \mathbb{Z}} : \xi_i \in \mathcal{A} \text{ for all } i \in \mathbb{Z}\}$  ( $\mathcal{A}^{\mathbb{Z}^+} = \{\xi = (\xi_i)_{i \in \mathbb{Z}^+} : \xi_i \in \mathcal{A} \text{ for all } i \in \mathbb{Z}^+\}$ ) be the two-sided (one-sided) infinite sequences equipped with the metric  $d(x, y) := (1 + k)^{-1}$ , where  $k = \min\{k \geq 0 : x_{|k|} \neq y_{|k|}\}$ . We call  $\mathcal{A}^{\mathbb{Z}}$  the *state space*.

The *left shift map* (simply *shift map*)  $\sigma_L : \mathcal{A}^{\mathbb{Z}} \rightarrow \mathcal{A}^{\mathbb{Z}}$  is defined by  $[\sigma_L(\xi)]_i := \xi_{i+1}$ ; the *right shift map*  $\sigma_R : \mathcal{A}^{\mathbb{Z}} \rightarrow \mathcal{A}^{\mathbb{Z}}$  is defined by  $[\sigma_R(\xi)]_i := \xi_{i-1}$  for any  $i \in \mathbb{Z}$ . The *full  $r$ -shift* (or simply  *$r$ -shift*) is the full shift over the alphabet  $\mathcal{A} = \{0, 1, \dots, r\}$  on the state space  $\mathcal{A}^{\mathbb{Z}}$ . Each sequence  $\xi \in \mathcal{A}^{\mathbb{Z}}$  is called a *point* of the state space. Points from the full 2-shift are also called *binary sequences*. A *cellular automaton* is a continuous map  $f^\infty : \mathcal{A}^{\mathbb{Z}} \rightarrow \mathcal{A}^{\mathbb{Z}}$  which commutes with the shift map, that is,  $f^\infty \sigma_L = \sigma_L f^\infty$ . For a cellular automaton  $f^\infty$ , a local rule  $f : \mathcal{A}^{2r+1} \rightarrow \mathcal{A}$  can be described as  $[f^\infty(x)]_i = f(x_{[i-r, i+r]})$ ,  $x \in \mathcal{A}^{\mathbb{Z}}$ .

Let  $\mathcal{F}$  be a collection of blocks over  $\mathcal{A}$  that we will consider as being the *forbidden blocks*. For any such  $\mathcal{F}$ , define  $X_{\mathcal{F}}$  to be the subset

of sequences in  $\mathcal{A}^{\mathbb{Z}}$  that do not contain any block in  $\mathcal{F}$ . A *shift space* is subset  $X$  of a full shift  $(\mathcal{A}^{\mathbb{Z}}, \sigma_L)$  such that  $X = X_{\mathcal{F}}$  for some collection  $\mathcal{F}$  of forbidden blocks over  $\mathcal{A}$ . For a given shift space there may be many collections  $\mathcal{F}$  describing it. When a shift space  $X$  is contained in a shift space  $Y$ , we say that  $X$  is a *subshift* of  $Y$ . More precisely, let  $\Sigma \subseteq \mathcal{A}^{\mathbb{Z}}$  be closed and invariant for  $\sigma_L$ , that is,  $\sigma_L(\Sigma) \subseteq \Sigma$ , then  $(\Sigma, \sigma_L)$  forms a subsystem of  $(\mathcal{A}^{\mathbb{Z}}, \sigma_L)$ . We call  $(\Sigma, \sigma_L)$  a subshift of the full shift  $(\mathcal{A}^{\mathbb{Z}}, \sigma_L)$ , denoted by  $(\Sigma, \sigma_L) \leq (\mathcal{A}^{\mathbb{Z}}, \sigma_L)$ . On each shift space there is a shift map from the space to itself. A type of mapping from one shift space to another is called a cellular automaton. We can make up infinitely many shift spaces by using different forbidden collections  $\mathcal{F}$ . Indeed, there are uncountably many shift spaces possible. As subsets of full shifts, these spaces share a common feature called shift invariance. A *shift of finite type* is a shift space that can be described by a finite set of forbidden blocks, that is, a shift space  $X$  having the form  $X_{\mathcal{F}}$  for some finite set  $\mathcal{F}$  of blocks. A shift of finite type is  $M$ -step (or has memory  $M$ ) if it can be described by a collection of forbidden blocks all of which have length  $M + 1$ .

One of the basic constructions in symbolic dynamics involves passing to a higher block shift, which provides an alternative description of the same shift space. Let  $X$  be a shift space over the alphabet  $\mathcal{A}$ , and  $\mathcal{A}_X^{[N]} = \mathcal{B}_N(X)$  be the collection of all allowed  $N$ -blocks in  $X$ . We can consider  $\mathcal{A}_X^{[N]}$  as an alphabet in its own right, and form the full shift  $(\mathcal{A}_X^{[N]})^{\mathbb{Z}}$ . Define the  $N^{\text{th}}$  *higher block code*  $\beta_N: X \rightarrow (\mathcal{A}_X^{[N]})^{\mathbb{Z}}$  by  $[\beta_N(\xi)]_i = \xi_{[i, i+N-1]}$ . Then the  $N^{\text{th}}$  higher block shift  $X^{[N]}$  or higher block presentation of  $X$  is the image  $X^{[N]} = \beta_N(X)$  in the full shift over  $\mathcal{A}_X^{[N]}$ .

Although in real life sequences of symbols are finite, it is often extremely useful to treat long sequences as infinite in one direction (one-sided infinite) or both directions (two-sided infinite). Directed graph theory provides a powerful tool for studying such infinite sequences. A fundamental method for constructing finite shifts starts with a finite, directed graph and produces the collection of all bi-infinite walks (i.e., sequences of edges) on the graph. A graph  $G$  consists of a finite set  $\mathcal{V} = \mathcal{V}(G)$  of vertices (or states) together with a finite set  $\mathcal{E} = \mathcal{E}(G)$  of edges. Each edge  $e \in \mathcal{E}(G)$  starts at a vertex denoted by  $i(e) \in \mathcal{V}(G)$  and terminates at a vertex  $t(e) \in \mathcal{V}(G)$ . Equivalently, the edge  $e$  has initial state  $i(e)$  and terminal state  $t(e)$ . We usually shorten  $\mathcal{V}(G)$  to  $V$  and  $\mathcal{E}(G)$  to  $\mathcal{E}$  when  $G$  is understood. A path  $\pi = e_1 e_2 \dots e_m$  on a graph  $G$  is a finite sequence of edges  $e_i$  from  $G$  such that  $t(e_i) = i(e_{i+1})$  for  $1 \leq i \leq m-1$ . The length of  $\pi = e_1 e_2 \dots e_m$  is  $|\pi| = m$ . The path  $\pi = e_1 e_2 \dots e_m$  starts at vertex  $i(\pi) = i(e_1)$  and terminates at vertex  $t(\pi) = t(e_m)$ , and  $\pi$  is a path

from  $i(\pi)$  to  $t(\pi)$ . A cycle is a path that starts and terminates at the same vertex. We say that a graph  $G$  is irreducible if for every ordered pair of vertices  $I$  and  $J$  there is a path in  $G$  starting at  $I$  and terminating at  $J$ . The following definitions developed in [1] are useful for directed graph theory.

**Definition 1.** Let  $G$  be a graph with vertex set  $\mathcal{V}$ . For vertices  $I, J \in \mathcal{V}$ , let  $A_{IJ}$  denote the number of edges in  $G$  with initial state  $I$  and terminal state  $J$ . Then the adjacency matrix of  $G$  is  $A = [A_{IJ}]$ , and its formation from  $G$  is denoted by  $A = A(G)$  or  $A = A_G$ .

**Definition 2.** Let  $G$  be a graph with edge set  $\mathcal{E}$  and adjacency matrix  $A$ . The edge shift  $X_G$  or  $X_A$  is the shift space over the alphabet  $\mathcal{A} = \mathcal{E}$  specified by

$$X_G = X_A = \{e = (e_i)_{i \in \mathbb{Z}} \in \mathcal{E}^{\mathbb{Z}} : t(e_i) = i(e_{i+1}) \text{ for all } i \in \mathbb{Z}\}.$$

### 3. Complex Shift Dynamics of Rules 30, 41, and 110

In this section we focus our attention on the discussion of complex shift dynamics of the special elementary cellular automaton rules 30, 41, and 110. We are dedicated to studying fractal structures and some complex Bernoulli shift dynamics of subsystems of these rules. It is worthwhile to mention that rule 30 was utilized to generate random sequences [9], rule 41 has complex shift dynamics, and rule 110 has proved to be capable of universal computation [10]. Therefore, it is very interesting to analyze the complex shift dynamics of these rules. We consider  $\mathcal{A} = \{0, 1\}$  and  $[f_R^\infty]_i = f_R(x_{[i-1, i+1]})$ , where  $R$  represents the rule number. In order to gain further insight on complex shift dynamics of these rules via an interval map from the viewpoint of symbolic dynamics, we consider the one-sided infinite symbolic sequences and represent them through the real number described by  $r_2(\xi) = \sum_{i=0}^{\infty} 2^{-(i+1)} \xi_i$ . Let  $\chi_R$  be the interval map corresponding to  $f_R^\infty$ . Therefore the following diagram commutes:

$$\begin{array}{ccc} \Sigma(\mathcal{A}) & \xrightarrow{f_R^\infty} & \Sigma(\mathcal{A}) \\ r_2 \downarrow & & \downarrow r_2 \\ [0, 1] & \xrightarrow{\chi_R} & [0, 1] \end{array}$$

Let  $I$  be the interval  $[0, 1]$ . The binary representation for a one-sided infinite symbolic sequence  $\xi_0 \xi_1 \dots$  is given by  $\phi = \sum_{i=0}^{\infty} \xi_i 2^{-(i+1)}$ . Denote by  $I_0$  the interval  $[0, 1/2]$ ,  $I_1$  the interval

$[1/2, 1]$ . For the Bernoulli shift  $b(\phi) = 2\phi \bmod 1$ , its inverse branches denoted by  $g$  are given by  $g_0: I \rightarrow I_0$  with  $g_0(\phi) = \phi/2$  and  $g_1: I \rightarrow I_1$  with  $g_1(\phi) = \phi/2 + 1/2$ . For a block  $\vec{\xi} \triangleq [\xi_0 \xi_1 \dots \xi_{I-1} \xi_I]$ , define  $g_{\vec{\xi}}(\phi) \triangleq g_{\xi_0} \circ g_{\xi_1} \circ \dots \circ g_{\xi_I}(\phi)$  and  $I_{\vec{\xi}} = g_{\vec{\xi}}([0, 1])$ .

We consider the case  $I \rightarrow \infty$ . To show the self-similarity of the interval map  $\chi_{30}$ ,  $\chi_{41}$ , and  $\chi_{110}$ , we present the following lemma.

**Lemma 1.** The interval map  $\chi_R$  satisfies the following general equation

$$\chi_R(\phi) = [\chi_R(g(\phi)) + f_R(\xi_* \xi_0 \xi_1)] 2^{-1} + [f_R(\xi_0 \xi_1 \xi_2) - f_R(\xi_* \xi_1 \xi_2)] 2^{-2}, \quad (1)$$

where  $\xi_*$  is determined by boundary conditions.

*Proof.* Let  $\phi = \sum_{i=0}^{\infty} \xi_i 2^{-(i+1)}$ . The interval map  $\chi_R$  yields

$$\chi_R(\phi) = f_R(\xi_* \xi_0 \xi_1) 2^{-1} + \sum_{i=1}^{\infty} f_R(\xi_{i-1} \xi_i \xi_{i+1}) 2^{-(i+1)}. \quad (2)$$

Hence, we have

$$\chi_R(g(\phi)) = f_R(\xi_* \xi_1 \xi_2) 2^{-1} + \sum_{i=2}^{\infty} f_R(\xi_{i-1} \xi_i \xi_{i+1}) 2^{-i}. \quad (3)$$

It follows from equations (2) and (3) that equation (1) holds. Thus, the proof is completed.  $\square$

### 3.1 Fractal Structures of Rules 30, 41, and 110

It is notable that the update law of rule 30 is given by

$$\begin{aligned} 000 &\rightarrow 0, & 001 &\rightarrow 1, & 010 &\rightarrow 1, & 011 &\rightarrow 1, \\ 100 &\rightarrow 1, & 101 &\rightarrow 0, & 110 &\rightarrow 0, & 111 &\rightarrow 0. \end{aligned}$$

Therefore, the following results are obtained.

**Theorem 1.** For the interval map  $\chi_{30}$ , when  $\xi_* = 0$ ,

$$\chi_{30}(\phi) = \begin{cases} \frac{1}{2} \chi_{30}(2\phi), & \text{if } \phi \in I_{00}, \\ \frac{1}{2} \chi_{30}(2\phi) + \frac{1}{2}, & \text{if } \phi \in I_{01}, \\ \frac{1}{2} \chi_{30}(2\phi - 1) + \frac{3}{4}, & \text{if } \phi \in I_{100}, \\ \frac{1}{2} \chi_{30}(2\phi - 1) + \frac{1}{4}, & \text{if } \phi \in I_{101}, \\ \frac{1}{2} \chi_{30}(2\phi - 1) + \frac{1}{4}, & \text{if } \phi \in I_{11}; \end{cases} \quad (4)$$

when  $\xi_* = 1$ ,

$$\chi_{30}(\phi) = \begin{cases} \frac{1}{2} \chi_{30}(2\phi) + \frac{1}{4}, & \text{if } \phi \in I_{000}, \\ \frac{1}{2} \chi_{30}(2\phi) + \frac{3}{4}, & \text{if } \phi \in I_{001}, \\ \frac{1}{2} \chi_{30}(2\phi) + \frac{1}{4}, & \text{if } \phi \in I_{01}, \\ \frac{1}{2} \chi_{30}(2\phi - 1), & \text{if } \phi \in I_1. \end{cases} \quad (5)$$

*Proof.* We only show the case when  $\xi_* = 0$ ; the proof when  $\xi_* = 1$  is similar. When  $\xi_* = 0$ , if  $\phi \in I_{00}$ , then  $\xi_0 = \xi_1 = 0$ ; it follows from equation (1) and the update law of rule 30 that

$\chi_{30}(\phi) = 1/2 \chi_{30}(2\phi)$ . Following the same analysis, if  $\phi \in I_{01}$ , then

$\chi_{30}(\phi) = 1/2 \chi_{30}(2\phi) + 1/2$ ; if  $\phi \in I_{100}$ , then

$\chi_{30}(\phi) = 1/2 \chi_{30}(2\phi - 1) + 3/4$ ; if  $\phi \in I_{101}$ , then

$\chi_{30}(\phi) = 1/2 \chi_{30}(2\phi - 1) + 1/4$ ; if  $\phi \in I_{11}$ , then

$\chi_{30}(\phi) = 1/2 \chi_{30}(2\phi - 1) + 1/4$ . Thus, equation (4) holds and the proof is completed.  $\square$

We can see from equations (4) and (5) that the interval map  $\chi_{30}$  exhibits some fractal structures, as illustrated in Figure 1, which to some extent reflect the complex shift dynamics of rule 30.

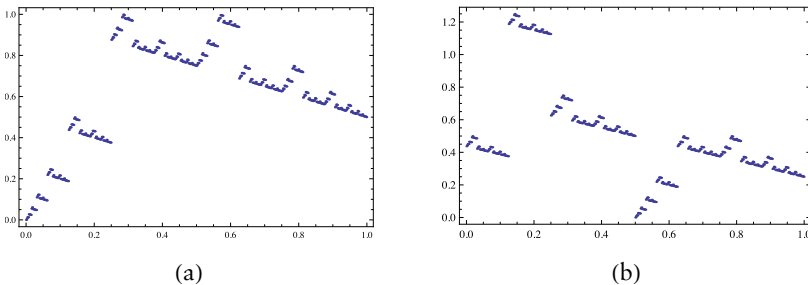


**Figure 1.** Fractal structures exhibited by the interval map  $\chi_{30}$  with different boundary conditions. (a)  $\xi_* = 0$ , (b)  $\xi_* = 1$ .

The update law of rule 41 is given by

$000 \rightarrow 1, \quad 001 \rightarrow 0, \quad 010 \rightarrow 0, \quad 011 \rightarrow 1,$

$100 \rightarrow 0, \quad 101 \rightarrow 1, \quad 110 \rightarrow 0, \quad 111 \rightarrow 0.$

Hence, we have the following results.

**Theorem 2.** For the interval map  $\chi_{41}$ , when  $\xi_* = 0$ ,

$$\chi_{41}(\phi) = \begin{cases} \frac{1}{2} \chi_{41}(2\phi) + \frac{1}{2}, & \text{if } \phi \in I_{00}, \\ \frac{1}{2} \chi_{41}(2\phi), & \text{if } \phi \in I_{01}, \\ \frac{1}{2} \chi_{41}(2\phi - 1) - \frac{1}{4}, & \text{if } \phi \in I_{100}, \\ \frac{1}{2} \chi_{41}(2\phi - 1) + \frac{1}{4}, & \text{if } \phi \in I_{101}, \\ \frac{1}{2} \chi_{41}(2\phi - 1) + \frac{1}{2}, & \text{if } \phi \in I_{110}, \\ \frac{1}{2} \chi_{41}(2\phi - 1) + \frac{1}{4}, & \text{if } \phi \in I_{111}; \end{cases} \quad (6)$$

when  $\xi_* = 1$ ,

$$\chi_{41}(\phi) = \begin{cases} \frac{1}{2} \chi_{41}(2\phi) + \frac{1}{4}, & \text{if } \phi \in I_{000}, \\ \frac{1}{2} \chi_{41}(2\phi) + \frac{3}{4}, & \text{if } \phi \in I_{001}, \\ \frac{1}{2} \chi_{41}(2\phi) + \frac{1}{2}, & \text{if } \phi \in I_{010}, \\ \frac{1}{2} \chi_{41}(2\phi) + \frac{3}{4}, & \text{if } \phi \in I_{011}, \\ \frac{1}{2} \chi_{41}(2\phi - 1), & \text{if } \phi \in I_1. \end{cases} \quad (7)$$

*Proof.* When  $\xi_* = 0$ , if  $\phi \in I_{00}$ , then  $\xi_0 = \xi_1 = 0$ ; it follows from equation (1) and the update law of rule 41 that  $\chi_{41}(\phi) = 1/2 \chi_{41}(2\phi) + 1/2$ . Carrying out the same analysis, if  $\phi \in I_{01}$ , then  $\chi_{41}(\phi) = 1/2 \chi_{41}(2\phi)$ ; if  $\phi \in I_{100}$ , then  $\chi_{41}(\phi) = 1/2 \chi_{41}(2\phi - 1) - 1/4$ ; if  $\phi \in I_{101}$ , then  $\chi_{41}(\phi) = 1/2 \chi_{41}(2\phi - 1) + 1/4$ ; if  $\phi \in I_{110}$ , then  $\chi_{41}(\phi) = 1/2 \chi_{41}(2\phi - 1) + 1/2$ ; if  $\phi \in I_{111}$ , then  $\chi_{41}(\phi) = 1/2 \chi_{41}(2\phi - 1) + 1/4$ . Thus, equation (6) holds. The proof of the case when  $\xi_* = 1$  is similar, and therefore equation (7) also holds. The proof is completed.  $\square$

Figure 2 illustrates the fractal structures exhibited by the interval map  $\chi_{41}$ , which in some sense demonstrates the complex shift dynamics of rule 41.

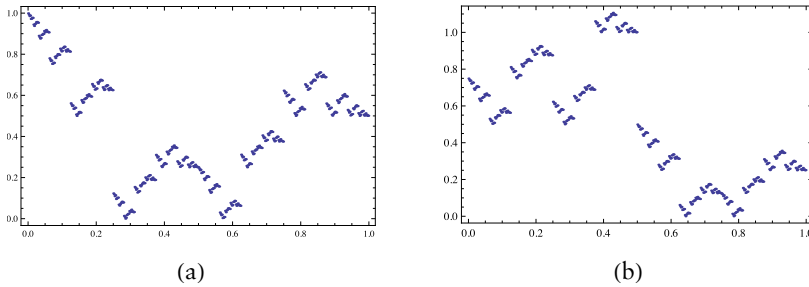


**Figure 2.** Fractal structures exhibited by the interval map  $\chi_{41}$  with different boundary conditions. (a)  $\xi_* = 0$ , (b)  $\xi_* = 1$ .

It is well known that the update law of universal rule 110 is given by

$$\begin{aligned} 000 &\rightarrow 0, & 001 &\rightarrow 1, & 010 &\rightarrow 1, & 011 &\rightarrow 1, \\ 100 &\rightarrow 0, & 101 &\rightarrow 1, & 110 &\rightarrow 1, & 111 &\rightarrow 0. \end{aligned}$$

Therefore, the following results are obtained.

**Theorem 3.** For the interval map  $\chi_{110}$ , when  $\xi_* = 0$ ,

$$\chi_{110}(\phi) = \begin{cases} \frac{1}{2} \chi_{110}(2\phi), & \text{if } \phi \in I_{00}, \\ \frac{1}{2} \chi_{110}(2\phi) + \frac{1}{2}, & \text{if } \phi \in I_{01}, \\ \frac{1}{2} \chi_{110}(2\phi - 1) + \frac{1}{2}, & \text{if } \phi \in I_{10}, \\ \frac{1}{2} \chi_{110}(2\phi - 1) + \frac{1}{2}, & \text{if } \phi \in I_{110}, \\ \frac{1}{2} \chi_{110}(2\phi - 1) + \frac{1}{4}, & \text{if } \phi \in I_{111}; \end{cases} \quad (8)$$

when  $\xi_* = 1$ ,

$$\chi_{110}(\phi) = \begin{cases} \frac{1}{2} \chi_{110}(2\phi), & \text{if } \phi \in I_{00}, \\ \frac{1}{2} \chi_{110}(2\phi) + \frac{1}{2}, & \text{if } \phi \in I_{010}, \\ \frac{1}{2} \chi_{110}(2\phi) + \frac{3}{4}, & \text{if } \phi \in I_{011}, \\ \frac{1}{2} \chi_{110}(2\phi - 1) + \frac{1}{4}, & \text{if } \phi \in I_{100}, \\ \frac{1}{2} \chi_{110}(2\phi - 1) + \frac{3}{4}, & \text{if } \phi \in I_{101}, \\ \frac{1}{2} \chi_{110}(2\phi - 1), & \text{if } \phi \in I_{11}. \end{cases} \quad (9)$$



*Proof.* We show the case when  $\xi_* = 0$ ; the proof when  $\xi_* = 1$  is similar. When  $\xi_* = 0$ , if  $\phi \in I_{00}$ , then  $\xi_0 = \xi_1 = 0$ ; it follows from equation (1) and the update law of rule 110 that  $\chi_{110}(\phi) = 1/2 \chi_{110}(2\phi)$ . Following the same analysis, if  $\phi \in I_{01}$ , then  $\chi_{110}(\phi) = 1/2 \chi_{110}(2\phi) + 1/2$ ; if  $\phi \in I_{10}$ , then  $\chi_{110}(\phi) = 1/2 \chi_{110}(2\phi - 1) + 1/2$ ; if  $\phi \in I_{110}$ , then  $\chi_{110}(\phi) = 1/2 \chi_{110}(2\phi - 1) + 1/2$ ; if  $\phi \in I_{111}$ , then  $\chi_{110}(\phi) = 1/2 \chi_{110}(2\phi - 1) + 1/4$ . Thus, equation (8) holds and the proof is completed.  $\square$

We can see some fractal structures exhibited by the interval map  $\chi_{110}$ , as illustrated in Figure 3.

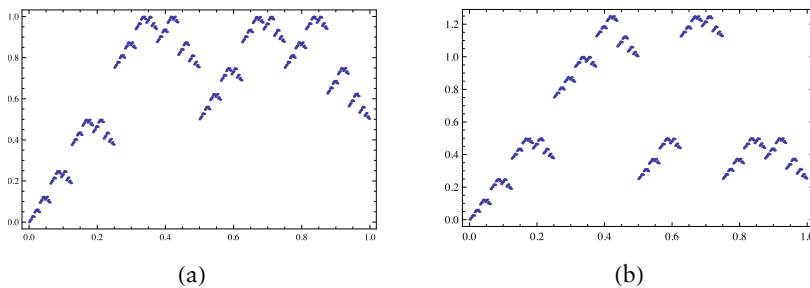


**Figure 3.** Fractal structures exhibited by the interval map  $\chi_{110}$  with different boundary conditions. (a)  $\xi_* = 0$ , (b)  $\xi_* = 1$ .

### 3.2 Subshifts of Rules 30, 41, and 110

Another good way to explore the complex shift dynamical behaviors is through subsystems that are better understood. To this end, in what follows we are dedicated to studying subshifts of rules 30, 41, and 110.

In fact, there are many closed invariant subsystems for these rules. Here we respectively present one simple subsystem for rules 30, 41, and 110 as follows.

- Here are the edges of directed graph  $G_1$ :  $e_1 = 0011\ 100$ ,  $e_2 = 0111\ 001$ ,  $e_3 = 1001\ 110$ ,  $e_4 = 1100\ 111$ ,  $e_5 = 1110\ 011$ .
- Here are the edges of directed graph  $G_2$ :  $e_1 = 0000\ 011$ ,  $e_2 = 0000\ 100$ ,  $e_3 = 0000\ 110$ ,  $e_4 = 0000\ 111$ ,  $e_5 = 0001\ 000$ ,  $e_6 = 0001\ 100$ ,  $e_7 = 0001\ 110$ ,  $e_8 = 0010\ 000$ ,  $e_9 = 0010\ 100$ ,  $e_{10} = 0011\ 000$ ,  $e_{11} = 0011\ 101$ ,  $e_{12} = 0100\ 000$ ,  $e_{13} = 0100\ 001$ ,  $e_{14} = 0100\ 100$ ,  $e_{15} = 0100\ 101$ ,  $e_{16} = 0101\ 001$ ,  $e_{17} = 0110\ 001$ ,  $e_{18} = 0111\ 010$ ,  $e_{19} = 1000\ 001$ ,  $e_{20} = 1000\ 010$ ,  $e_{21} = 1000\ 110$ ,  $e_{22} = 1000\ 111$ ,  $e_{23} = 1001\ 000$ ,  $e_{24} = 1001\ 010$ ,  $e_{25} = 1010\ 010$ ,  $e_{26} = 1100\ 011$ ,  $e_{27} = 1101\ 001$ ,  $e_{28} = 1110\ 100$ .
- Here are the edges of directed graph  $G_3$ :  $e_1 = 0001\ 001$ ,  $e_2 = 0001\ 110$ ,  $e_3 = 0010\ 011$ ,  $e_4 = 0011\ 010$ ,  $e_5 = 0011\ 011$ ,

$e_6 = 0011100, e_7 = 0011101, e_8 = 0100110, e_9 = 0110100,$   
 $e_{10} = 0110111, e_{11} = 0111000, e_{12} = 0111010, e_{13} = 0111011,$   
 $e_{14} = 0111110, e_{15} = 1000100, e_{16} = 1000111, e_{17} = 1001101,$   
 $e_{18} = 1010011, e_{19} = 1011100, e_{20} = 1011101, e_{21} = 1011111,$   
 $e_{22} = 1100010, e_{23} = 1100011, e_{24} = 1101001, e_{25} = 1101110,$   
 $e_{26} = 1101111, e_{27} = 1110001, e_{28} = 1110100, e_{29} = 1110111,$   
 $e_{30} = 1111000, e_{31} = 1111010, e_{32} = 1111011, e_{33} = 1111100,$   
 $e_{34} = 1111101.$

The edges constitute the higher 7-block edge shift, which is a 1-step shift of finite type, as depicted in Figures 4, 5, and 6. All bi-infinite walks on the graph constitute the closed invariant subsystem denoted by  $\Lambda_1, \Lambda_2$ , and  $\Lambda_3$ . The graph  $G_i$  is strongly connected and its corresponding adjacency matrix  $A_i$  is irreducible. According to the well-known Perron–Frobenius theory, we know that the topological entropy  $h(X_{G_i}) = \log \lambda_{A_i}(G_i) > 0$ , where the positive eigenvalue  $\lambda_{A_i}(G_i)$  is the Perron eigenvalue of irreducible matrix  $A_i$  ( $i = 1, 2, 3$ ). Hence  $f_{30}^\infty, f_{41}^\infty, f_{110}^\infty$  is topological mixing on  $\Lambda_1, \Lambda_2$ , and  $\Lambda_3$ , respectively. Moreover, there exists a Bernoulli shift attractor on  $\Lambda_i$  ( $i = 1, 2, 3$ ) as  $(f_{30}^\infty)^3|_{\Lambda_1} = \sigma_L|_{\Lambda_1}, (f_{41}^\infty)^3|_{\Lambda_2} = \sigma_R|_{\Lambda_2}, (f_{110}^\infty)^3|_{\Lambda_3} = \sigma_R^2|_{\Lambda_3}$  holds. In order to perfectly characterize the Bernoulli shift, we introduce the two parameters  $\tau$  and  $\sigma$  developed in [5] to predict its dynamic evolution, where  $\tau$  denotes the relevant forward time- $\tau$  map and  $\sigma$  denotes the shift related with  $\tau$ . As an example for illustration, we take a special symbolic sequence

$$\begin{aligned}\vec{\xi}_1 &= [0111001110], \\ \vec{\xi}_2 &= [10001110100100000110001], \text{ and} \\ \vec{\xi} &= [0110100110111000111010]\end{aligned}$$

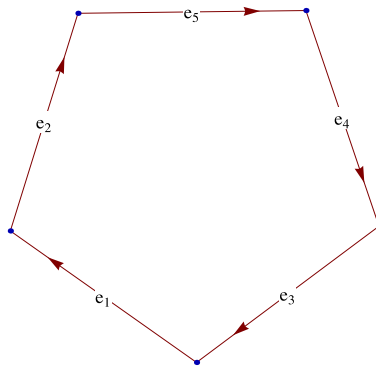


**Figure 4.** Graph representation of a subsystem for rule 30 (graph  $G_1$ ).

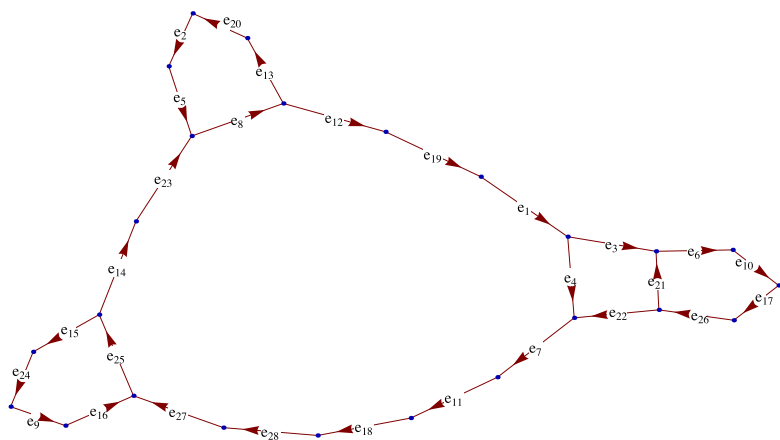


**Figure 5.** Graph representation of a subsystem for rule 41 (graph  $G_2$ ).

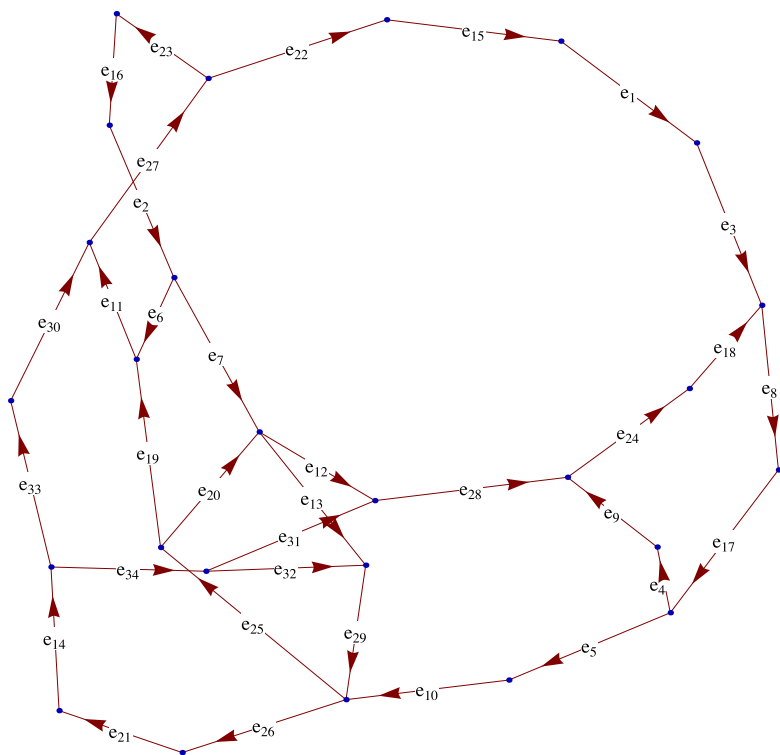


**Figure 6.** Graph representation of a subsystem for rule 110 (graph  $G_3$ ).

with periodic boundary conditions that are extracted from a cycle of the directed graphs  $G_1$ ,  $G_2$ , and  $G_3$ , respectively. For the same initial configuration  $\vec{\xi}_i$  ( $i = 1, 2, 3$ ), we can see in Figure 7 that the dynamics evolving under  $f_{30}^\infty$  exhibit the Bernoulli shift with  $\sigma = 1$  and  $\tau = 3$ , which means shift the symbolic sequence to the left by one pixel after every three evolution steps. In Figure 8 we can see that the dynamics evolving under  $f_{41}^\infty$  exhibit the Bernoulli shift with  $\sigma = -1$  and  $\tau = 3$ , which means shift the symbolic sequence to the right by one pixel after every three evolution steps. In Figure 9 we can see that the dynamics evolving under  $f_{110}^\infty$  exhibit the Bernoulli shift with  $\sigma = -2$  and  $\tau = 3$ , which means shift the symbolic sequence to the right by two pixels after every three evolution steps.

In fact, many complex Bernoulli shifts exist that are components of attractors of rules 30, 41, and 110. In order to illustrate this, we consider the finite symbolic sequences with the length denoted by  $L$ . For different  $L$ , we pick out one symbolic sequence as an initial configuration, which is extracted from one of the periodic attractors under rules 30, 41, and 110, respectively. We can see that complex Bernoulli shifts exist for each initial configuration, as illustrated in Tables 1 through 3. This also to some extent perfectly characterizes the complex shift dynamics of rules 30, 41, and 110.

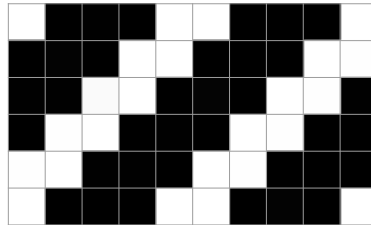


**Figure 7.** Bernoulli shift extracted every three steps from the dynamic evolution of  $f_{30}^\infty$  with the initial configuration  $\vec{\xi} = [0111001110]$ .

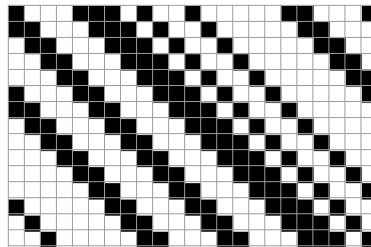


**Figure 8.** Bernoulli shift extracted every three steps from the dynamic evolution of  $f_{41}^\infty$  with the initial configuration  $\vec{\xi} = [10001110100100000110001]$ .

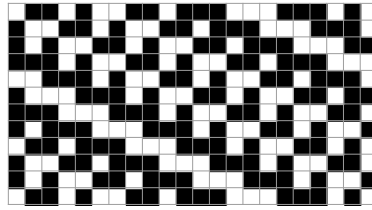


**Figure 9.** Bernoulli shift extracted every three steps from the dynamic evolution of  $f_{110}^\infty$  with the initial configuration  $\vec{\xi} = [0110100110111000111010]$ .

$L$	Initial Configuration	Period	$\sigma$	$\tau$
11	111000011110	154	1	56
12	000001111110	102	4	68
13	1000110000001	832	1	192
14	01111101110011	1428	1	1326
15	011000111000011	1455	-2	679

**Table 1.** List of complex Bernoulli shifts of rule 30 for different  $L$  ranging from  $L = 11$  to  $L = 15$ .

$L$	Initial Configuration	Period	$\sigma$	$\tau$
10	0000001001	40	2	24
11	00000000001	44	-1	12
12	000000100011	36	-1	15
13	0100000011000	117	1	18
14	00000000000001	28	2	12
15	000000000000001	60	-1	16
16	0010000100000000	176	-2	22

**Table 2.** List of complex Bernoulli shifts of rule 41 for different  $L$  ranging from  $L = 10$  to  $L = 16$ .

$L$	Initial Configuration	Period	$\sigma$	$\tau$
11	11101110011	110	1	50
12	011111000111	18	-2	3
13	1111111000100	351	1	189
14	01101111111110	91	-2	13
15	001111100110001	295	-3	118
16	1111100010011000	32	2	4
17	00111001100111110	578	-1	238
18	111000001101000011	81	2	9

**Table 3.** List of complex Bernoulli shifts of rule 110 for different  $L$  ranging from  $L = 11$  to  $L = 18$ .

#### 4. Concluding Remarks

---

This paper has demonstrated some complex shift dynamics of rules 30, 41, and 110 from the viewpoint of symbolic dynamics. By associating an interval map with these rules, it is shown that the interval map exhibits some degree of self-similarity. Based on directed graph theory, it is demonstrated that rules 30, 41, and 110 exhibit Bernoulli shifts and are topologically mixing on one of their own subsystems. Last but not least, for the finite symbolic sequences with periodic boundary conditions, many complex Bernoulli shifts are explored from the periodic attractors.

#### Acknowledgments

---

The authors would like to thank the handling editor and anonymous referees for their constructive suggestions for revision of the manuscript. This work is supported by the Research Foundation of Hangzhou Dianzi University (KYS075609067) and Hainan Nature Science Foundation (110007).

#### References

---

- [1] D. Lind and B. Marcus, *An Introduction to Symbolic Dynamics and Coding*, Cambridge: Cambridge University Press, 1995.
- [2] B. P. Kitchens, *Symbolic Dynamics: One-Sided, Two-Sided and Countable State Markov Shifts*, Berlin: Springer-Verlag, 1998.
- [3] C. Marr and M.-T. Hütt, "Outer-Totalistic Cellular Automata on Graphs," *Physics Letters A*, 373(5), 2009 pp. 546–549. doi:10.1016/j.physleta.2008.12.013.
- [4] H. Yue, H. Guan, J. Zhang, and C. Shao, "Study on Bi-Direction Pedestrian Flow using Cellular Automata Simulation," *Physica A*, 389(3), 2010 pp. 527–539. doi:10.1016/j.physa.2009.09.035.
- [5] L. O. Chua, V. I. Sbitnev, and S. Yoon, "A Nonlinear Dynamics Perspective of Wolfram's New Kind of Science. Part IV: From Bernoulli Shift to  $1/f$  Spectrum," *International Journal of Bifurcation and Chaos*, 15(4), 2005 pp. 1045–1183. doi:10.1142/S0218127405012995.
- [6] L. O. Chua, V. I. Sbitnev, and S. Yoon, "A Nonlinear Dynamics Perspective of Wolfram's New Kind of Science. Part V: Fractals Everywhere," *International Journal of Bifurcation and Chaos*, 15(12), 2005 pp. 3701–3849. doi:10.1142/S0218127405014775.
- [7] L. O. Chua, V. I. Sbitnev, and S. Yoon, "A Nonlinear Dynamics Perspective of Wolfram's New Kind of Science. Part VI: From Time-Reversible Attractors to the Arrow of Time," *International Journal of Bifurcation and Chaos*, 16(5), 2006 pp. 1097–1373. doi:10.1142/S0218127406015544.

- [8] L. O. Chua, J. Guan, V. I. Sbitnev, and J. Shin, “A Nonlinear Dynamics Perspective of Wolfram’s New Kind of Science. Part VII: Isles of Eden,” *International Journal of Bifurcation and Chaos*, 17(9), 2007 pp. 2839–3012. doi:10.1142/S0218127407019068.
- [9] S. Wolfram, “Random Sequence Generation by Cellular Automata,” *Advances in Applied Mathematics*, 7(2), 1986 pp. 123–169. doi:10.1016/0196-8858(86)90028-X.
- [10] M. Cook, “Universality in Elementary Cellular Automata,” *Complex Systems*, 15(1), 2004 pp. 1–40.